148 mm, 20× reduction, negatives) containing all of the supplementary material for the papers in this issue may be obtained from the Journals Department, American Chemical Society, 1155 16th St., N.W., Washington, D. C. 20036. Remit check or money order for $4.00 for photocopy or $2.00 for microfiche, referring to code number INORG-74-2819.

Contribution from Dow Chemical U. S. A., Midland, Michigan 48640

Cyclomer Complexes. II. Crystal Structure of a 2:1 Octahydrate Complex of 1,4,7,10-Tetraoxacyclododecane with Sodium Hydroxide

F. P. BOER, M. A. NEUMAN, F. P. van REMOORTERE,* and E. C. STEINER[1]

Received February 27, 1974 AIC40135S

The crystal structure of the complex $NaOH \cdot 2C_8H_{16}O_4 \cdot 8H_2O$, where $C_8H_{16}O_4$ is 1,4,7,10-tetraoxacyclododecane, has been determined by a single-crystal three-dimensional X-ray diffraction study. This substance crystallizes in space group *Pbcn*, with lattice constants $a = 14.794 \pm 0.004$, $b = 15.845 \pm 0.004$, and $c = 23.960 \pm 0.006$ Å ($Z = 8$). The intensities of 4781 unique reflections were measured on a Picker four-circle diffractometer (θ–2θ scan, Cu Kα radiation) and the structure was solved by Patterson and Fourier methods. Full-matrix least-squares refinement of the coordinates and anisotropic temperature factors of the Na, O, and C atoms converged at a final $R_1 = 6.6\%$ for 2926 reflections above background. The methylene hydrogens were located but their positions were not refined. The sodium ion forms an eight-coordinated sandwich complex of approximate D_4 symmetry with two polyether rings, each of which manifests approximate C_4 symmetry. The oxygen atoms are arranged at the corners of a square antiprism at an average Na–O distance of 2.485 Å. The hydroxide ion is associated with the water molecules to form infinite sheets of linked four- and five-membered rings extending in planes perpendicular to the *c* axis.

Introduction

Crystallographic investigations of 1,4,7,10-tetraoxacyclododecane complexes with alkali halide salts have revealed some novel structural properties.[2] In these compounds, species of D_4 symmetry are formed, where the oxygen atoms of two cyclomer molecules occupy the vertices of a square antiprism centered on the cation. These units form organic layers through the crystal, while the halide ions are associated with water molecules in infinite two-dimensional hydrogen-bonded networks. These aqueous layers have an interesting structure based on six-membered rings. As a result of this organization of the crystal lattice the positive and negative ions are completely separated.

The discovery of these structures raised the question of whether the basic D_4 unit and the presence of discrete, alternating aqueous and organic strata might be unique to the alkali halide complexes $MX \cdot 2C_8H_{16}O_4 \cdot 5H_2O$ or occur generally in a broader class of compounds. The preparation of a crystalline complex of 1,4,7,10-tetraoxacyclododecane with NaOH afforded an opportunity to explore this question further and to extend our knowledge of the structural systematics of cyclomer chelates with alkali ions as applied to a chemical of major industrial significance. We report here a three-dimensional X-ray diffraction study of $NaOH \cdot 2C_8H_{16}O_4 \cdot 8H_2O$ which establishes that the structural principles of the alkali halide series are effectively retained in the caustic complex. However, as might be expected from the differences in stoichiometry, the detailed arrangement of atoms within the hydrogen-bonded aqueous layer is fundamentally dissimilar in the caustic structure and is in fact based on five-membered rings.

Experimental Section

Crystals of $NaOH \cdot 2C_8H_{16}O_4 \cdot 8H_2O$ are readily obtained by cooling slightly a saturated aqueous solution of NaOH, to which 2 equiv of cyclomer had been added. The crystals are colorless rectangular prisms, elongated markedly along the *b* axis and flattened along *a*.

A crystal of dimensions 0.12 × 0.50 × 0.20 mm (along *a*, *b*, and *c*, respectively) was selected and mounted in a 0.3-mm diameter thin-walled glass capillary with the *b* axis of the crystal approximately parallel to the capillary axis. The crystal was then aligned and examined by photographic methods on a Weissenberg goniometer to determine the space group and preliminary lattice constants. The reciprocal lattice symmetry D_{2h} and the reflection conditions $0kl$ ($k = 2n$), $h0l$ ($l = 2n$), and $hk0$ ($h + k = 2n$) recorded on the $h0l$ and $h1l$ Weissenberg levels establish the space group uniquely as *Pbcn* (No. 60, D_{2h}^{14}). The crystal was then carefully centered on a Picker four-circle goniostat, and the dimensions of the orthorhombic cell were calculated by least-squares refinement of the setting angles of 11 reflections with Cu Kα radiation (λ 1.5418 Å). The lattice parameters $a = 14.794 \pm 0.004$, $b = 15.845 \pm 0.004$, and $c = 23.960 \pm 0.006$ Å (at 25°) are consistent with a calculated density of 1.232 g cm^{-3} for mol wt 536.55 and $Z = 8$. The estimated standard deviations of the lattice constants, as computed in the least-squares analysis, were a factor of 10 better than the errors assigned above, which reflect our experience with systematic errors and reproducibility of results under different experimental conditions. The presence of 8 formula units/unit cell does not impose any requirements on the symmetry of the complex.

Intensity data were gathered using the θ–2θ scan mode of the diffractometer with Ni-filtered Cu Kα radiation. The takeoff angle of the tube was 3°, and a counter aperture 6.0 × 6.0 mm was placed 30 cm from the crystal; 1.5 mm diameter incident- and exit-beam collimators were used to restrict stray radiation. The scan speed was 2°/min over 2θ angles of $2° + \Delta$, where Δ is the separation of the Kα doublet; this range was sufficient to allow for the observed mosaic spread of the crystal. Two stationary-crystal, stationary-counter background counts of 10 sec were taken at each end of the scan. Attenuators were used to prevent the count rate from exceeding 12,000/sec. The reciprocal lattice was recorded to near the instrumental limit ($\sin\theta = 0.906$) and a total of 4781 independent reflections was measured. A test reflection (614) monitored after every 50 measurements showed fair stability; the root-mean-square deviation in intensity was 1.5% and some measurements deviated by as much as 4%. An error $\sigma(I) = [(0.02I)^2 + N_o + k^2N_b]^{1/2}$ was assigned to the net intensity $I = N_o - kN_b$ of each reflection in order to establish the weights $w(F) = 4F^2/\sigma^2(F^2)$ for subsequent least-squares refinement, where the quantity $\Sigma w(|F_o| - |F_c|)^2$ was minimized. Here N_o is the gross count, N_b is the background count, k is the ratio of scan time to background time, and the F^2 are the intensities corrected for Lorentz and polarization effects. The 1852 reflections for which

(1) The crystallographic work was carried out by F. P. Boer, M. A. Neuman, and F. P. van Remoortere; E. C. Steiner synthesized the complex.

(2) (a) F. P. van Remoortere and F. P. Boer, *Inorg. Chem.*, 13, 2071 (1974); (b) H. W. Rinn, E. C. Steiner, and F. P. Boer, unpublished results.

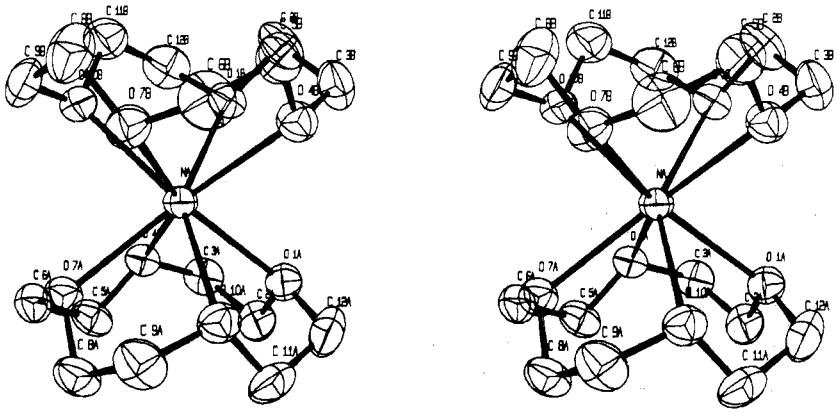

Figure 1. Three-dimensional stereopair view of the $[Na^+(C_8H_{16}O_4)_2]$ moiety. The thermal ellipsoids are drawn at the 40% probability level.

$I < 0$ or $I/\sigma(I) < 3.3$ were denoted absent and omitted from the refinement. The linear absorption coefficient for Cu Kα radiation is 10.85 cm^{-1}. No corrections were made for absorption; transmission factors were estimated to range from about 0.80 to 0.88. Finally a scale factor and overall temperature factor ($B_o = 4.9$ A^2) were estimated by Wilson's method.

Solution and Refinement of the Structure

That the solution of the crystal structure required the location of at least 34 unique light atoms—more, should some of these occur at special positions—was recognized from the outset. Accordingly, direct methods appeared to offer an attractive approach to solving the phase problem, and the programs REL[3] and MAGIC[4] were in turn applied to the data. A satisfactory solution was not obtained, and an examination of the output from MAGIC indicated that the relatively low values of the normalized structure factors (E's) for k odd reflections were the probable source of the difficulty. Before pursuing statistical methods any further we chose to examine a Patterson function and this approach eventually solved the phase problem.

Normal-sharpened coefficients[5] were calculated and used to compute[6] a three-dimensional Patterson function. As expected from the weakness of the k odd reflections, this map showed a very strong peak at 0, $^1/_2$, 0 and an approximate mirror plane at $y = {}^1/_4$. From its Harker interactions, the sodium ion was located at approximately $^1/_4$, $^1/_8$, z ($z \simeq 0.012$), or very nearly on the b glide. Assuming a square-antiprismatic geometry as found in the $[Na^+(C_8H_{16}O_4)_2][Cl^- \cdot 5H_2O]$ complex, we now attempted to determine the orientation of the cyclomer complex from the Na→O (ether) vectors. The point symmetry of a square antiprism is D_{4d}, and it was recognized at this time that if one mirror plane of the antiprism was oriented perpendicular to x the sodium and oxygen atoms could not contribute to the k odd reflections. Interestingly, this lead proved to be false and it will be seen below that the *water* structure exhibits a noncrystallographic mirror plane at $x = {}^1/_4$. The key to the correct solution was obtained when a set of intramolecular Na→O vectors fitting a square antiprism was identified and the Na→O intermolecular vectors derived from this set were shown to be uniformly consistent with the Patterson function. The Na→O vector pattern could not, however, distinguish between structures related by a mirror plane at $y = {}^1/_8$ arising from a noncrystallographic twofold axis through the sodium parallel to a. This ambiguity was resolved by a structure factor calculation:[7-9] the correct image gave $R_1 = 0.577$ and $R_2 = 0.666$, whereas the false image gave $R_1 = 0.633$ and $R_2 = 0.731$. The quantities R_1 and R_2 are defined as $\Sigma||F_o| - |F_c||/\Sigma|F_o|$ and $\{\Sigma w(F_o - F_c)^2/\Sigma wF_o^2\}^{1/2}$, respectively, and refer here to the subset of 1189 observed reflections in the region $\sin\theta < 0.6$. For the correct image R_1 had values of 0.470 for the k odd reflections alone and 0.627 for the reflections with k even. The remaining carbon and oxygen atoms were now located by Fourier methods;[6] the presence of four water oxygens on crystallographic twofold axes raised the number of unique nonhydrogen atoms to 36.

In the first stage of refinement, position parameters, and isotropic temperature factors of the Na, O, and C atoms were varied by full-matrix least squares using the truncated set of 1189 reflections. After four cycles R_1 and R_2 were reduced to 0.125 and 0.176, respectively, and a difference Fourier was generated.[6] From the molecular structure at this stage, positions were calculated for the methylene hydrogens under the assumption that these were symmetrically disposed in normal planes containing the bisectors of the C–C–O angles with H–C–H angles of 109.5° and C–H distances of 1.020 A. The latter value is shorter than the presumed true internuclear separation, about 1.091 A, to correct for the bias of the centroid of electron density from the proton toward the bonding region.[9] The difference map showed peaks at or near each of these calculated positions, with peak heights ranging from 0.29 to 0.62 e A^{-3}. In neither this nor in subsequent difference Fouriers were we able to locate the hydrogens directly bonded to oxygen atoms, most likely because the H_2O and OH^- species exhibit larger amplitudes of thermal motion than the ring atoms. With the inclusion of the 32 methylene hydrogens at their calculated positions in the structure factor calculation we were able to reduce the R factors further to $R_1 = 0.116$ and $R_2 = 0.141$ after one additional cycle of isotropic refinement.[7] (The hydrogen positions were not varied and a single isotropic temperature factor, which *was* varied, was assigned to all hydrogens.)

Refinement assuming anisotropic thermal motion for the nonhydrogen atoms, which required variation of 310 independent parameters, was carried out in blocks of 238 variables (the maximum for our full-matrix program[7] on a CDC 3800 (64K words) computer). Care was taken to ensure that all variables from the logical structural units, *i.e.*, the cyclomer rings or the aqueous layer, were permitted to refine simultaneously at least twice. Hydrogen positions were recalculated to take into account shifts by the heavier atoms. Also, two intense reflections (002 and 200) which appeared to be affected by secondary extinction and one weak reflection (004) located in a strong white radiation streak were removed from the data set. After five cycles, refinement converged at final values of $R_1 = 6.6\%$ and $R_2 = 7.8\%$ for 2926 observed reflections. By the last cycle the mean parameter shift had been reduced to 0.02σ, and no individual shift exceeded 0.25σ. In the final difference Fourier the highest positive peak was 0.40 e A^{-3}, and the lowest negative density was −0.36 e A^{-3}. The standard deviations on bond distances and angles were computed[10] from the variance-covariance matrix obtained in the final least-squares cycle.

Final atomic parameters and their standard deviations as computed from the least-squares analysis are given in Table I. Observed and calculated structure factors are available on request.[11] The root-mean-square components of thermal motion along the principal

(3) R. E. Long, Ph.D. Thesis, University of California at Los Angeles, 1966; D. Sayre, *Acta Crystallogr.*, 5, 60 (1952).

(4) R. B. K. Dewar and A. L. Stone, Program MAGIC and auxiliary links, University of Chicago, 1968.

(5) W. N. Lipscomb in "The Technique of Organic Chemistry," Vol. 1, A. Weissberger, Ed., Interscience, New York, N. Y., 1960, pp 1695-1697.

(6) J. Gvildys, "Two- and Three-Dimensional Crystallographic Fourier Summation Program," based on MIFRI, Program Library B-149, Argonne National Laboratory, Applied Mathematics Division, Argonne, Ill., April 13, 1965.

(7) J. Gvildys, "A Fortran Crystallographic Least-Squares Refinement Program," based on ORFLS, Program Library 14E7043, Argonne National Laboratory, March 31, 1967.

(8) Atomic scattering factors were taken from "International Tables for X-Ray Crystallography," Vol. III, Kynoch Press, Birmingham, England, 1962, pp 201-209. Hydrogen scattering factors are, however, from ref 9.

(9) R. F. Stewart, E. R. Davidson, and W. T. Simpson, *J. Chem. Phys.*, 42, 3175 (1965).

(10) J. Gvildys, "ANL FFE, a Fortran Crystallographic Function and Error Program," based on ORFFE, Program Library B 115, Argonne National Laboratory, Sept 17, 1964.

(11) See paragraph at end of paper regarding supplementary material.

Table I. Atomic Parameters and Standard Deviations[a]

Atom	x/a	y/b	z/c	$10^5\beta_{11}$	$10^5\beta_{22}$	$10^5\beta_{33}$	$10^5\beta_{12}$	$10^5\beta_{13}$	$10^5\beta_{23}$
Na	0.2536 (1)	0.1247 (1)	0.0115 (1)	423 (7)	345 (6)	127 (2)	5 (7)	−2 (5)	8 (4)
O(1A)	0.3823 (2)	0.1405 (2)	0.0788 (1)	520 (16)	437 (16)	188 (7)	−8 (14)	−42 (9)	30 (8)
C(2A)	0.4089 (3)	0.0647 (3)	0.1050 (2)	502 (25)	551 (27)	238 (12)	27 (23)	−95 (15)	72 (14)
C(3A)	0.4008 (3)	−0.0048 (3)	0.0638 (2)	460 (24)	560 (23)	236 (12)	158 (22)	17 (15)	35 (14)
O(4A)	0.3104 (2)	−0.0146 (2)	0.0434 (1)	499 (15)	406 (14)	161 (6)	24 (13)	28 (8)	13 (7)
C(5A)	0.2516 (3)	−0.0585 (3)	0.0807 (2)	737 (28)	360 (21)	225 (10)	18 (24)	77 (17)	86 (13)
C(6A)	0.1571 (3)	−0.0436 (3)	0.0623 (2)	667 (28)	401 (24)	215 (10)	−127 (23)	33 (14)	−11 (13)
O(7A)	0.1340 (2)	0.0438 (2)	0.0615 (1)	530 (16)	405 (15)	175 (6)	−11 (13)	34 (9)	−12 (8)
C(8A)	0.1111 (3)	0.0764 (3)	0.1149 (2)	635 (28)	522 (26)	193 (10)	−7 (24)	141 (14)	−15 (14)
C(9A)	0.1172 (3)	0.1697 (3)	0.1115 (2)	555 (27)	573 (28)	267 (11)	123 (25)	142 (17)	−52 (14)
O(10A)	0.2053 (2)	0.1981 (2)	0.0960 (1)	593 (18)	394 (14)	169 (6)	20 (13)	10 (9)	−10 (8)
C(11A)	0.2675 (3)	0.1982 (3)	0.1412 (2)	842 (35)	515 (22)	159 (10)	19 (27)	−36 (14)	−99 (13)
C(12A)	0.3607 (4)	0.2073 (3)	0.1170 (2)	800 (32)	463 (22)	271 (13)	−122 (24)	−186 (19)	−33 (14)
O(1B)	0.3712 (2)	0.1144 (2)	−0.0626 (1)	561 (18)	440 (15)	194 (6)	15 (13)	57 (9)	31 (9)
C(2B)	0.3923 (3)	0.1909 (3)	−0.0901 (2)	644 (31)	519 (27)	321 (13)	19 (24)	192 (17)	67 (16)
C(3B)	0.3868 (3)	0.2596 (3)	−0.0486 (2)	567 (29)	522 (26)	300 (13)	−165 (23)	80 (16)	−1 (16)
O(4B)	0.2993 (2)	0.2667 (2)	−0.0228 (1)	510 (16)	413 (15)	194 (7)	8 (13)	−5 (9)	26 (8)
C(5B)	0.2354 (4)	0.3096 (3)	−0.0558 (2)	816 (36)	365 (21)	261 (12)	5 (23)	−89 (17)	34 (13)
C(6B)	0.1440 (3)	0.2913 (3)	−0.0328 (2)	673 (34)	488 (27)	319 (14)	148 (25)	−10 (17)	40 (16)
O(7B)	0.1233 (2)	0.2033 (2)	−0.0313 (1)	533 (17)	498 (16)	195 (6)	4 (15)	−53 (9)	24 (9)
C(8B)	0.0942 (3)	0.1707 (3)	−0.0831 (2)	566 (30)	676 (31)	344 (15)	43 (25)	−151 (18)	−10 (18)
C(9B)	0.1032 (3)	0.0779 (3)	−0.0812 (2)	686 (34)	619 (30)	267 (13)	−209 (27)	−201 (16)	21 (16)
O(10B)	0.1951 (2)	0.0509 (2)	−0.0712 (1)	617 (18)	484 (16)	161 (6)	−91 (15)	−31 (9)	6 (9)
C(11B)	0.2508 (4)	0.0523 (2)	−0.1193 (2)	1039 (40)	654 (28)	183 (10)	−166 (32)	69 (19)	−81 (14)
C(12B)	0.3464 (4)	0.4882 (3)	−0.1004 (2)	821 (33)	591 (30)	259 (13)	143 (29)	138 (19)	−51 (15)
W(1)	0.0734 (2)	0.3789 (2)	0.1876 (1)	848 (24)	684 (20)	251 (8)	−66 (19)	26 (11)	−1 (11)
W(2)	0.1150 (3)	0.1342 (2)	0.2960 (2)	1115 (34)	756 (25)	489 (13)	−9 (23)	2 (16)	29 (14)
W(3)	0.2606 (3)	0.0498 (2)	0.2499 (2)	1947 (43)	598 (20)	351 (10)	7 (26)	66 (19)	56 (14)
W(4)	0.2606 (3)	0.2470 (3)	0.2962 (2)	1992 (44)	705 (22)	239 (8)	−81 (26)	19 (16)	−74 (11)
W(5)	0.2513 (2)	0.3842 (2)	0.2294 (1)	825 (23)	639 (20)	357 (10)	4 (19)	−23 (13)	−28 (11)
W(6)	0.3940 (4)	0.1345 (3)	0.2943 (2)	1554 (48)	1098 (32)	731 (20)	147 (33)	−166 (24)	77 (20)
W(7)	0.4281 (2)	0.3844 (2)	0.1893 (1)	927 (25)	575 (32)	229 (8)	21 (18)	−56 (11)	−14 (10)
W(8)	0	0.0199 (3)	0.25	1071 (39)	452 (25)	404 (16)	0	145 (21)	0
W(9)	0	0.2467 (3)	0.25	1010 (40)	459 (24)	417 (15)	0	193 (20)	0
W(10)	0.5	0.0135 (3)	0.25	1174 (43)	553 (29)	465 (18)	0	−163 (23)	0
W(11)	0.5	0.2504 (3)	0.25	1167 (44)	467 (25)	445 (16)	0	−290 (22)	0

[a] Standard errors obtained from the least-squares refinement are given in parentheses. Temperature factors are in the form $\exp[-(h^2\beta_{11} + k^2\beta_{22} + l^2\beta_{33} + 2hk\beta_{12} + 2hl\beta_{13} + 2kl\beta_{23})]$.

Table II. Root-Mean-Square Thermal Displacements (A) along Principal Axes[a]

Atom	Axis 1	Axis 2	Axis 3	Atom	Axis 1	Axis 2	Axis 3
Na	0.191	0.210	0.217	C(6B)	0.220	0.293	0.309
O(1A)	0.217	0.236	0.257	O(7B)	0.218	0.251	0.263
C(2A)	0.201	0.261	0.296	C(8B)	0.220	0.293	0.339
C(3A)	0.199	0.257	0.293	C(9B)	0.187	0.273	0.351
O(4A)	0.211	0.224	0.244	O(10B)	0.213	0.233	0.278
C(5A)	0.190	0.256	0.304	C(11B)	0.215	0.276	0.359
C(6A)	0.210	0.246	0.289	C(12B)	0.214	0.291	0.334
O(7A)	0.218	0.228	0.251	W(1)	0.268	0.287	0.316
C(8A)	0.193	0.258	0.300	W(2)	0.309	0.352	0.378
C(9A)	0.187	0.285	0.310	W(3)	0.269	0.324	0.466
O(10A)	0.218	0.227	0.258	W(4)	0.249	0.310	0.471
C(11A)	0.186	0.275	0.309	W(5)	0.283	0.301	0.326
C(12A)	0.199	0.263	0.344	W(6)	0.352	0.415	0.474
O(1B)	0.217	0.237	0.268	W(7)	0.253	0.271	0.325
C(2B)	0.211	0.255	0.348	W(8)	0.240	0.303	0.380
C(3B)	0.206	0.278	0.311	W(9)	0.241	0.286	0.389
O(4B)	0.221	0.238	0.245	W(10)	0.265	0.321	0.403
C(5B)	0.211	0.260	0.318	W(11)	0.244	0.278	0.426

[a] Ordered on increasing magnitude.

axes, as defined by the anisotropic thermal parameters, are summarized in Table II. The directions of these axes may be inferred from Figures 1–3, where ellipsoids of constant probability are used to represent the thermal motion.[12]

Discussion

The crystal structure of $[Na^+(C_8H_{16}O_4)_2][OH^-\cdot 8H_2O]$ (I), as determined in this study, is organized on chemical and geometrical relationships analogous to those operating[2a] in the series of alkali halide complexes $[M^+(C_8H_{16}O_4)_2][X^-\cdot 5H_2O]$, henceforth referred to as II for MX = NaCl. The configurations of the $[Na^+(C_8H_{16}O_4)_2]$ units (Figure 1) are virtually identical in I and II, and the unusual feature of a crystal separated into alternating organic and aqueous layers, containing the positive and negative charges, respectively, is again present (Figure 4).[12] In both cases, these strata lie in planes perpendicular to the longest crystal axis (c = 23.960 in I, a = 22.122 in II) and repeat at intervals of half the unit cell length in this direction. While these general structural principles have been maintained, the detailed construction of the individual strata differ in certain respects.

Description of the Cyclomer Layer. Within each individual organic layer, the cyclomer complexes are aligned in a parallel fashion. This feature is common to structures I and II. The orientations of the $[Na^+(C_8H_{16}O_4)_2]$ units are also remarkably similar; in each case one of the twofold axes of the D_4 units is parallel to the shortest cell translation and the normals to the square faces of the antiprism form nearly equal angles with respect to the longest cell translation (13° 20′ to c in I, 14° 42′ to a in II). The presence of screw diads along the long dimension results in a herring-bone pattern (Figure 4) where the normals to the antiprism faces alternate in direction at intervals of half the cell translation.

The arrangement of $[Na^+(C_8H_{16}O_4)_2]$ units within a layer is analogous to the ideal close-packing of spheres in two dimensions. This model is followed quite closely in the sodium hydroxide complex where the six nearest neighbors occur at similar distances. (Na^+-Na^+ interionic distances are 7.923 Å for the two neighbors related by the b glide; 8.312 and 8.498 Å for ions generated by inversion centers at $\frac{1}{2}$, 0, 0

(12) C. K. Johnson, "ORTEP: A Fortran Thermal-Ellipsoid Plot Program for Crystal Structure Illustrations," Report ORNL-3794, Oak Ridge National Laboratory, Oak Ridge, Tenn., June 1965.

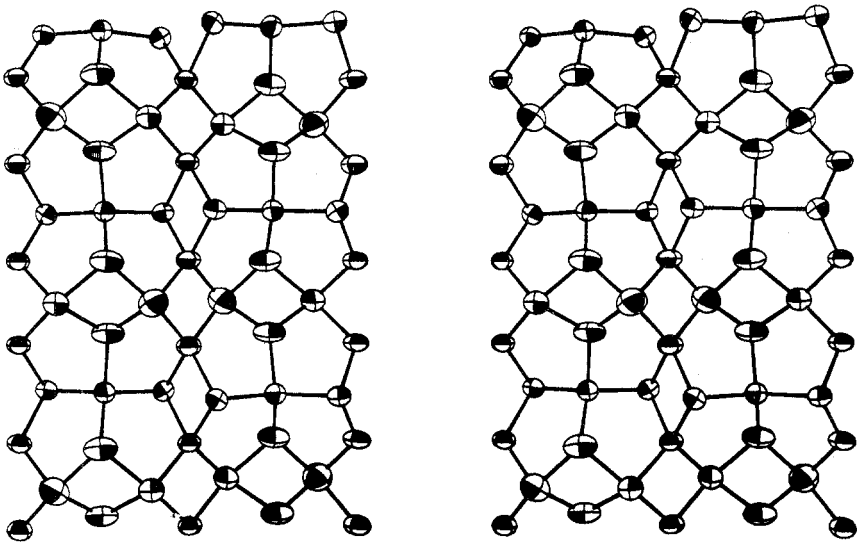

Figure 2. Three-dimensional stereopair view of the aqueous layer in $[Na^+(C_8H_{16}O_4)_2][OH^-\cdot 8H_2O]$ with thermal ellipsoids drawn at 50% probability.

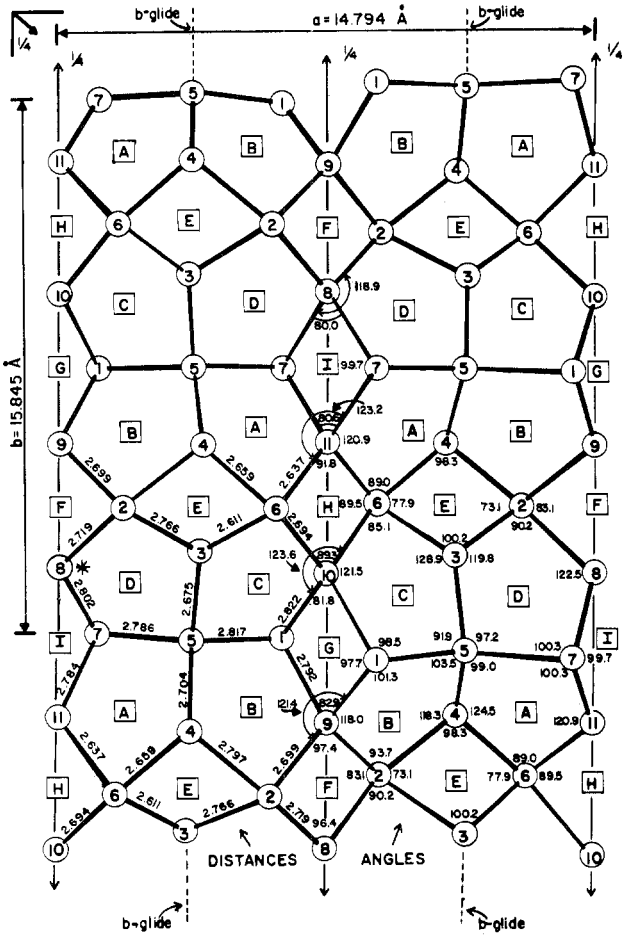

Figure 3. The atom and ring labels, symmetry elements, and bond distances and angles. The origin is labeled by an asterisk, the a axis runs from left to right, and b from bottom to top.

and 0, 0, 0, respectively; and 8.413 Å for the two sodiums related by the screw diad parallel to x.) The hexagonal packing pattern was more seriously distorted in II as indicated by a more widely variant set of Na^+-Na^+ separations (compare 7.571 Å for sodium ions related by centers at 0, 0, 0 and 0, 0, $^1/_2$; 7.829 Å for those across the centers at 0, $^1/_2$, $^1/_2$ and 0, $^1/_2$, 0; and 9.544 Å for the two neighbors produced by the cell translations along b). The configuration of the $[Na^+(C_8H_{16}O_4)_2]$ units and the type of packing found in the layers formed by these species results in structures where only the methylene groups of the cyclomer complexes are presented to the aqueous layer.

Description of the Aqueous Layer. The water molecules and hydroxide ions form symmetrical networks of hydrogen bonds based on five-membered rings (Figures 2 and 3) that extend in infinite sheets parallel to (001). The 16 unique O···O contacts at hydrogen-bonded distances contained in this system range from 2.611 ± 0.007 to 2.822 ± 0.005 Å (Table III), compared to the 2.822 ± 0.006, 2.878 ± 0.004, and 2.934 ± 0.004 Å observed in II. These values, together with the infrared spectra,[13] indicate that some stronger hydrogen bonds are present in the NaOH complex. However, these 16 hydrogen-bonded distances are insufficient to accommodate the 17 hydrogen atoms demanded by the stoichiometry. As the hydrogen atoms in the aqueous layer were not found in this study, no final conclusion can be drawn as to the location of the hydrogen atom not participating in the network, nor can the hydroxide oxygen be identified. However, the band at 3642 cm^{-1} observed in the polarized Raman[13] spectra of a single crystal is strongest in the α_{zz} spectrum indicating that the nonbonded O-H is directed approximately along the z (crystallographic c) axis. An examination of Figure 3 shows that the shortest group of O···H-O distances occurs at O(6). This may well be the principal site of the negative charge associated with the hydroxide oxygen since a charged oxygen atom is particularly receptive to the protons of the adjacent water molecules and is expected to give rise to strong hydrogen bonds. In view of the high symmetry of the structure the possibility that the hydrogen atoms and the negative charge are distributed among multiple sites should, however, not be overlooked.

A prominent structural feature is the arrangement of four five-membered rings (labeled A, B, C, and D in Figure 3) to form a subunit of approximate C_{2v} symmetry. Although

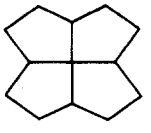

(13) V. B. Carter, personal communication.

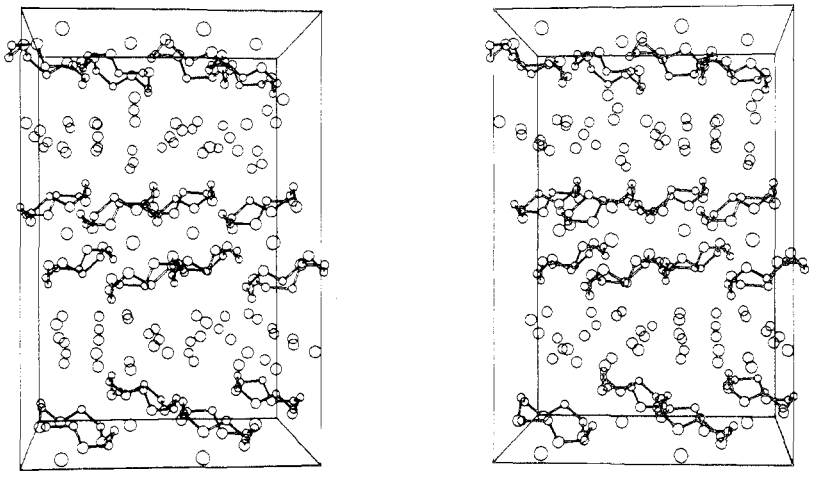

Figure 4. Three-dimensional stereopair view of a unit cell of $[Na^+(C_8H_{16}O_4)_2][OH^-\cdot 8H_2O]$. The origin is at the lower right front corner of the box defining the volume $0 < x < 1, 0 < y < 1, 0 < z < 1$. The c axis is vertical and b is horizontal.

Table III. Selected Distances (A) and Angles (deg) in the Water Layer[a]

Distances

W(1)-W(5)	2.817 (5)	W(4)-W(5)	2.704 (5)
W(1)-W(9)	2.792 (5)	W(4)-W(6)	2.659 (7)
W(1)-W(10)(I)	2.822 (5)	W(5)-W(7)	2.786 (5)
W(2)-W(3)	2.766 (6)	W(6)-W(10)	2.694 (6)
W(2)-W(4)	2.797 (6)	W(6)-W(11)	2.637 (6)
W(2)-W(8)	2.719 (5)	W(7)-W(8)(I)	2.802 (5)
W(2)-W(9)	2.699 (5)	W(7)-W(11)	2.784 (5)
W(3)-W(5)(II)	2.675 (5)		
W(3)-W(6)	2.611 (7)		

Angles

W(1)-W(5)-W(9)	101.3 (0.1)	W(6)-W(3)-W(4)	77.9 (0.2)
W(1)-W(5)-W(10)(I)	98.5 (0.1)	W(6)-W(3)-W(10)	85.1 (0.2)
W(1)-W(9)-W(10)(I)	97.7 (0.1)	W(6)-W(3)-W(11)	130.0 (0.2)
W(2)-W(3)-W(4)	73.1 (0.2)	W(6)-W(4)-W(10)	156.3 (0.2)
W(2)-W(3)-W(8)	90.2 (0.2)	W(6)-W(4)-W(11)	89.0 (0.2)
W(2)-W(3)-W(9)	130.3 (0.2)	W(6)-W(10)-W(11)	89.5 (0.2)
W(2)-W(4)-W(8)	155.2 (0.2)	W(7)-W(5)-W(8)	100.3 (0.1)
W(2)-W(4)-W(9)	93.7 (0.2)	W(7)-W(5)-W(11)	100.3 (0.1)
W(2)-W(8)-W(9)	83.1 (0.2)	W(7)-W(8)-W(11)	99.7 (0.1)
W(3)-W(2)-W(5)(II)	119.8 (0.2)	W(8)-W(2)-W(2)(III)	96.4 (0.2)
W(3)-W(2)-W(6)	100.2 (0.2)	W(8)-W(2)-W(7)(II)	122.5 (0.1)
W(3)-W(5)(II)-W(6)	128.9 (0.2)	W(8)-W(2)-W(7)(IV)	118.9 (0.1)
W(4)-W(2)-W(5)	118.3 (0.2)	W(8)-W(7)(II)-W(7)(IV)	80.0 (0.2)
W(4)-W(2)-W(6)	98.3 (0.2)	W(9)-W(1)-W(1)(III)	82.9 (0.2)
W(4)-W(5)-W(6)	124.5 (0.2)	W(9)-W(1)-W(2)	118.0 (0.1)
W(5)-W(1)-W(3)(I)	91.9 (0.2)	W(9)-W(1)-W(2)(III)	121.4 (0.1)
W(5)-W(1)-W(4)	103.5 (0.2)	W(9)-W(2)-W(2)(III)	97.4 (0.2)
W(5)-W(1)-W(7)	139.0 (0.2)	W(10)-W(1)(II)-W(1)(VI)	81.8 (0.2)
W(5)-W(3)(I)-W(4)	133.1 (0.2)	W(10)-W(1)(II)-W(6)	121.5 (0.1)
W(5)-W(3)(I)-W(7)	97.2 (0.2)	W(10)-W(1)(II)-W(6)(V)	123.6 (0.1)
W(5)-W(4)-W(7)	99.0 (0.2)	W(10)-W(6)-W(6)(V)	89.3 (0.3)
		W(11)-W(6)-W(6)(V)	91.8 (0.3)
		W(11)-W(6)-W(7)	120.9 (0.1)
		W(11)-W(6)-W(7)(V)	123.2 (0.1)
		W(11)-W(7)-W(7)(V)	80.6 (0.2)

[a] Standard errors calculated from the variance-covariance matrix obtained in the final least-squares cycle are given in parentheses. Transformations are as follows: (I) $^1/_2 - x, ^1/_2 + y, z$; (II) $^1/_2 - x, -^1/_2 + y, z$; (III) $-x, y, ^1/_2 - z$; (IV) $-^1/_2 + x, -^1/_2 + y, ^1/_2 - z$; (V) $1 - x, y, ^1/_2 - z$; (VI) $^1/_2 + x, -^1/_2 + y, ^1/_2 - z$.

this structural unit appears in some polyhedral hydrates of the clathrate type,[14] in the present case it forms a basic building block of a two-dimensional network. Extension of this network in the a direction arises by application of twofold axes parallel to b passing through the outer atoms of the subunit (W(8), W(9), W(10), and W(11)). As a consequence, the planar four-membered rings, F, G, H, and I are generated along the diads. Multiplication of this subunit in the b direction is accomplished by the b glide, which, when coupled with the approximate noncrystallographic mirror plane at $x = ^1/_4$, reduces to the pseudotranslation of $b/2$ encountered

(14) M. vanStackelberg and H. R. Muller, *Z. Elektrochem.*, 58, 25 (1954); R. K. McMullan and G. A. Jeffrey, *J. Chem. Phys.*, 31, 1231 (1959); 37, 2231 (1962); 42, 2725 (1964); D. Feil and G. A. Jeffrey, *ibid.*, 35, 1863 (1961); M. Bonamico, G. A. Jeffrey, and R. K. McMullan, *ibid.*, 37, 2219 (1962).

Table IV. Least-Squares Planes and Dihedral Angles for Water Layer[a]

A. Planes

	Ring								
	A	B	C	D	E	F	G	H	I
Atom 1	W(4)	W(1)	W(1)(II)	W(2)	W(2)	W(2)	W(1)	W(11)	W(7)
Atom 2	W(5)	W(2)	W(5)(II)	W(3)	W(3)	W(8)	W(9)	W(6)	W(11)
Atom 3	W(6)	W(4)	W(3)	W(8)	W(4)	W(9)	W(1)(III)	W(10)	W(8)(I)
Atom 4	W(7)	W(5)	W(6)	W(5)(II)	W(6)	W(2)(III)	W(10)(I)	W(6)(V)	W(7)(V)
Atom 5	W(11)	W(9)	W(10)	W(7)(II)					
m_1	3.915	−3.916	1.096	−1.015	0.248	8.050	11.973	8.288	11.941
m_2	8.160	8.250	−7.214	−7.234	−5.244	0	0	0	0
m_3	19.535	19.448	21.259	21.253	22.606	−20.102	14.072	19.847	−14.143
d	8.641	6.645	5.607	5.062	5.745	−5.026	3.518	9.106	2.435
$\Delta d(1)$	0.181	−0.158	−0.278	0.143	0.272	0	0	0	0
$\Delta d(2)$	−0.041	−0.230	0.377	−0.374	−0.292	0	0	0	0
$\Delta d(3)$	−0.252	0.133	−0.367	0.108	−0.280	0	0	0	0
$\Delta d(4)$	−0.130	0.002	0.110	0.398	0.300	0	0	0	0
$\Delta d(5)$	0.243	0.253	0.158	−0.275					

B. Angles, Deg

Plane 1	Plane 2	Angle	Plane 1	Plane 2	Angle	Plane 1	Plane 2	Angle	Plane 1	Plane 2	Angle
A	A(V)	61.98	C	C(V)	54.17	B	B(III)	62.75	D	I(II)	62.08
A	B	30.70	C	D	8.18	B	C(I)	59.82	E	F	38.52
A	C	59.43	C	E	8.48	B	D	59.97	E	H	37.73
A	C(I)	62.00	C	G(II)	62.53	B	D(I)	62.35	F	G	87.00
A	D(I)	59.58	C	H	39.07	B	E	53.92	F	I(II)	86.78
A	E	52.90	D	D(III)	54.33	B	F	34.40	H	G(II)	87.90
A	H	34.55	D	E	9.30	B	G	74.78	H	I	88.10
A	I	74.48	D	F	38.60						

[a] The planes are defined by the equation $m_1x + m_2y + m_3z = d$. Roman numerals correspond to the symmetry transformations described in Table III.

in the Patterson function (*vide supra*). A fifth four-membered ring, labeled E, is thereby generated, and this links with rings F and H to form chains of four-membered rings in the *a* direction. Rings A, B, C, D, and E are markedly nonplanar. Best planes through these atoms are described in Table IV, and the unique dihedral angles formed between planes sharing a common atom or edge are also listed there. In *projection* (Figure 3) the water structure shows approximate *p4m* symmetry with horizontal mirror planes (perpendicular to *b*) passing through the W(5) oxygens, in addition to the vertical mirror planes at $x = 1/4$. However, a comparison of the dihedral angles listed in Table IV, or alternatively a close examination of the stereopair diagram (Figure 2), shows that in three dimensions this horizontal mirror exists only at a very low level of approximation. On the other hand, the interplanar angles (Table IV) related by the *vertical* mirror plane agree remarkably well—in fact considerably better than the distances and angles formed between individual atoms (Table III).

The 11 independent oxygen atoms in the structural subunit described above may be classified into three different types according to their functional role. Atoms W(1), W(3), W(4), and W(7) are hydrogen bonded to three other oxygen atoms only and join two five-membered rings with a four-membered one. The remaining six atoms form hydrogen bonds to four neighbors, but while W(2), W(6), W(8), W(9), W(10), and W(11) act as the spiro links in infinite chains of four-membered rings (and simultaneously join adjacent five-membered rings), atom W(5) is uniquely situated at the junction of four-five membered cycles.

Description of the Cyclomer Metal Complex. The geometry of the $[Na^+(C_8H_{16}O_4)_2]$ sandwich is shown in three dimensions in Figure 1 and its metrical parameters are listed in Tables V–VIII. Figure 5 summarizes the dimensions of the square antiprism formed by the eight ether oxygens. Although no symmetry is imposed by the space group, the com-

Table V. Selected Interatomic Distances (Å) for the Cyclomer Complex (A)[a]

Sodium–Oxygen Distances		**Sodium–Carbon Distances**	
Na–O(1A)	2.508 (3)	Na–C(2A)	3.347 (4)
Na–O(4A)	2.483 (3)	Na–C(5A)	3.343 (4)
Na–O(7A)	2.491 (3)	Na–C(8A)	3.342 (4)
Na–O(10A)	2.441 (3)	Na–C(11A)	3.325 (4)
Na–O(1B)	2.493 (3)	Na–C(2B)	3.352 (5)
Na–O(4B)	2.489 (3)	Na–C(5B)	3.356 (5)
Na–O(7B)	2.514 (3)	Na–C(8B)	3.351 (5)
Na–O(10B)	2.459 (3)	Na–C(11B)	3.338 (5)
Carbon–Carbon Bonds		Na–C(3A)	3.245 (5)
C(2A)–C(3A)	1.484 (6)	Na–C(6A)	3.261 (4)
C(5A)–C(6A)	1.486 (6)	Na–C(9A)	3.212 (5)
C(8A)–C(9A)	1.484 (6)	Na–C(12A)	3.257 (5)
C(11A)–C(12A)	1.502 (6)	Na–C(3B)	3.245 (5)
C(2B)–C(3B)	1.476 (6)	Na–C(6B)	3.275 (5)
C(5B)–C(6B)	1.489 (6)	Na–C(9B)	3.231 (5)
C(8B)–C(9B)	1.477 (7)	Na–C(12B)	3.244 (5)
C(11B)–C(12B)	1.485 (7)		
Carbon–Oxygen Bonds		**Oxygen–Oxygen Intra-ring Distances**	
C(2A)–O(1A)	1.411 (5)	O(1A)–O(4A)	2.809 (4)
C(12A)–O(1A)	1.436 (5)	O(4A)–O(7A)	2.802 (4)
C(3A)–O(4A)	1.432 (5)	O(7A)–O(10A)	2.788 (4)
C(5A)–O(4A)	1.427 (5)	O(10A)–O(1A)	2.804 (4)
C(6A)–O(7A)	1.427 (5)	O(1B)–O(4B)	2.804 (4)
C(8A)–O(7A)	1.421 (5)	O(4B)–O(7B)	2.798 (4)
C(9A)–O(10A)	1.428 (5)	O(7B)–O(10B)	2.807 (4)
C(11A)–O(10A)	1.421 (5)	O(10B)–O(1B)	2.801 (4)
C(2B)–O(1B)	1.413 (5)		
C(12B)–O(1B)	1.426 (5)	**Oxygen–Oxygen Inter-ring Distances**	
C(3B)–O(4B)	1.438 (5)	O(1A)–O(1B)	3.418 (4)
C(5B)–O(4B)	1.409 (5)	O(1A)–O(4B)	3.380 (4)
C(6B)–O(7B)	1.428 (5)	O(4A)–O(1B)	3.384 (4)
C(8B)–O(7B)	1.411 (5)	O(4A)–O(10B)	3.395 (4)
C(9B)–O(10B)	1.446 (5)	O(7A)–O(7B)	3.371 (4)
C(11B)–O(10B)	1.417 (5)	O(7A)–O(10B)	3.308 (4)
		O(10A)–O(7B)	3.284 (4)
		O(10A)–O(4B)	3.349 (4)

[a] Standard errors calculated from the variance–covariance matrix obtained in the final least-squares cycle are given in parentheses.

Table VI. Selected Interatomic Angles for the Cyclomer Complex (deg)[a]

Vertex	Atom 1	Atom 2	Angle	Vertex	Atom 1	Atom 2	Angle
Na	O(1A)	O(4A)	68.5 (0.1)	C(2A)	C(5A)	C(11A)	88.6 (0.3)
	O(1A)	O(10A)	69.0 (0.1)	C(5A)	C(2A)	C(8A)	91.1 (0.3)
	O(4A)	O(7A)	68.6 (0.1)	C(8A)	C(5A)	C(11A)	90.0 (0.3)
	O(7A)	O(10A)	68.8 (0.1)	C(11A)	C(2A)	C(8A)	91.3 (0.3)
	O(1B)	O(4B)	68.5 (0.1)	C(2B)	C(5B)	C(11B)	89.1 (0.3)
	O(1B)	O(10B)	68.9 (0.1)	C(5B)	C(2B)	C(8B)	91.0 (0.3)
	O(4B)	O(7B)	68.0 (0.1)	C(8B)	C(5B)	C(11B)	89.1 (0.3)
	O(7B)	O(10B)	68.6 (0.1)	C(11B)	C(2B)	C(8B)	90.7 (0.3)
	O(1A)	O(1B)	86.2 (0.1)				
	O(1A)	O(4B)	85.2 (0.1)	C(3A)	C(6A)	C(12A)	89.9 (0.3)
	O(4A)	O(1B)	85.7 (0.1)	C(6A)	C(3A)	C(9A)	90.0 (0.3)
	O(4A)	O(10B)	86.8 (0.1)	C(9A)	C(6A)	C(12A)	90.2 (0.3)
	O(7A)	O(7B)	84.7 (0.1)	C(12A)	C(3A)	C(9A)	89.9 (0.3)
	O(7A)	O(10B)	83.9 (0.1)	C(3B)	C(6B)	C(12B)	90.0 (0.3)
	O(10A)	O(4B)	85.6 (0.1)	C(6B)	C(3B)	C(9B)	90.1 (0.3)
	O(10A)	O(7B)	83.0 (0.1)	C(9B)	C(6B)	C(12B)	89.7 (0.3)
	O(1A)	O(7A)	106.3 (0.1)	C(12B)	C(3B)	C(9B)	90.2 (0.3)
	O(4A)	O(10A)	105.5 (0.1)				
	O(1B)	O(7B)	106.1 (0.1)	O(1A)	C(2A)	C(12A)	113.9 (0.4)
	O(4B)	O(10B)	105.0 (0.1)	C(2A)	O(1A)	C(3A)	108.3 (0.4)
	O(1A)	O(7B)	142.7 (0.1)	C(3A)	C(2A)	O(4A)	112.5 (0.3)
	O(1A)	O(10B)	146.4 (0.1)	O(4A)	C(3A)	C(5A)	114.1 (0.3)
	O(4A)	O(4B)	144.4 (0.1)	C(5A)	O(4A)	C(6A)	108.1 (0.3)
	O(4A)	O(7B)	145.7 (0.1)	C(6A)	C(5A)	O(7A)	112.5 (0.3)
	O(7A)	O(4B)	144.8 (0.1)	O(7A)	C(6A)	C(8A)	113.5 (0.3)
	O(7A)	O(1B)	143.6 (0.1)	C(8A)	O(7A)	C(9A)	107.3 (0.4)
	O(10A)	O(1B)	145.7 (0.1)	C(9A)	C(8A)	O(10A)	112.6 (0.4)
	O(10A)	O(10B)	142.4 (0.1)	O(10A)	C(9A)	C(11A)	113.1 (0.3)
				C(11A)	O(10A)	C(12A)	107.5 (0.3)
O(1A)	Na	C(12A)	108.3 (0.2)	C(12A)	C(11A)	O(1A)	112.4 (0.3)
	Na	C(2A)	114.4 (0.2)				
				O(1B)	C(2B)	C(12B)	112.8 (0.4)
O(4A)	Na	C(3A)	109.0 (0.2)	C(2B)	O(1B)	C(3B)	107.9 (0.4)
	Na	C(5A)	114.8 (0.2)	C(3B)	C(2A)	O(4B)	113.3 (0.4)
				O(4B)	C(3B)	C(5B)	113.5 (0.3)
O(7A)	Na	C(6A)	109.6 (0.2)	C(5B)	O(4B)	C(6B)	107.9 (0.4)
	Na	C(8A)	114.6 (0.2)	C(6B)	C(5B)	O(7B)	113.2 (0.4)
				O(7B)	C(6B)	C(8B)	113.6 (0.4)
O(10A)	Na	C(9A)	109.4 (0.2)	C(8B)	O(7B)	C(9B)	108.1 (0.4)
		C(11A)	116.3 (0.2)	C(9B)	C(8B)	O(10B)	112.6 (0.4)
				O(10B)	C(9B)	C(11B)	114.0 (0.4)
O(1B)	Na	C(12B)	108.6 (0.2)	C(11B)	O(10B)	C(12B)	107.8 (0.4)
	Na	C(2B)	115.4 (0.2)	C(12B)	C(11B)	O(1B)	114.3 (0.4)
O(4B)	Na	C(3B)	108.5 (0.2)				
	Na	C(5B)	116.1 (0.2)				
O(7B)	Na	C(6B)	109.3 (0.2)				
	Na	C(8B)	114.3 (0.2)				
O(10B)	Na	C(9B)	108.9 (0.2)				
	Na	C(11B)	116.3 (0.2)				
O(1A)	O(4A)	O(10A)	88.6 (0.3)				
O(4A)	O(1A)	O(7A)	91.0 (0.3)				
O(7A)	O(4A)	O(10A)	89.1 (0.3)				
O(10A)	O(1A)	O(7A)	91.4 (0.3)				
O(1B)	O(4B)	O(10B)	88.9 (0.3)				
O(4B)	O(1B)	O(7B)	91.1 (0.3)				
O(7B)	O(4B)	O(10B)	88.9 (0.3)				
O(10B)	O(1B)	O(7B)	91.0 (0.3)				

[a] Standard errors calculated from the variance-covariance matrix obtained in the final least-squares cycle are given in parentheses.

plex approximates the point group D_4 fairly well and is in fact somewhat less distorted from this ideal geometry in the present structure than in II.[2a] This point is illustrated by a comparison of the dihedral angles formed by the square faces (1.6° in I *vs* 3.0° in II—see Table VIII) and is also evident in a narrower variation in the O···O inter-ring contacts, which range between 3.303 and 3.549 Å in II but only between 3.284 and 3.418 Å here. The varying degrees of distortion from ideal geometry support our previous suggestion that deviations from D_4 symmetry are not intrinsic to the complex but rather result from packing forces.

One unexpected result for which we have no explanation is that two of the Na-O distances, those to O(10A) (2.441 ± 0.003 Å) and to O(10B) (2.459 ± 0.003 Å) appear to be significantly shorter than the other six (average 2.497 Å) and also shorter than the Na-O distances in II (average 2.496 Å). Despite these differences, the four oxygen atoms from each ring appear to be coplanar within experimental error (Table VIII). As measured along the normals, the distances from the best planes through these atoms to the Na^+ ion are in reasonably close agreement (1.497 Å for ring A and 1.505 Å for ring B) and are somewhat shorter than the corresponding distance of 1.528 Å found for II. As permitted by the basic D_4 symmetry of the complex, there are two chemically distinct types of carbon atoms;[1] we have designated those labeled 3, 6, 9, and 12 as type α, and those labeled 2, 5, 8 and 11 as type β. The α carbons lie near planes (Table VIII) 1.969 Å (ring A) and 1.987 Å (ring B) distant from the cation,

Table VII. Torsion Angles (deg) in 12-Membered Rings[a]

	Ring A	Ring B
C(12)-O(1)-C(2)-C(3)	162.18	161.35
C(1)-C(2)-C(3)-O(4)	−59.90	−58.73
C(2)-C(3)-O(4)-C(5)	−78.97	−80.22
C(3)-O(4)-C(5)-C(6)	164.63	163.92
O(4)-C(5)-C(6)-O(7)	−58.88	−57.95
C(5)-C(6)-O(7)-C(8)	−80.68	−80.83
C(6)-O(7)-C(8)-C(9)	162.55	162.20
O(7)-C(8)-C(9)-O(10)	−59.12	−59.63
C(8)-C(9)-O(10)-C(11)	−79.65	−80.05
C(9)-O(10)-C(11)-C(12)	165.73	163.15
O(10)-C(11)-C(12)-O(1)	−58.82	−56.48
C(11)-C(12)-O(1)-C(2)	−79.68	−81.53

[a] The sign convention is the one recommended by W. Klyne and V. Prelog, *Experientia*, 16, 521 (1960).

Table VIII. Least-Squares Planes in the Cyclomer Complex[a,b]

	Plane					
	1	2	3	4	5	6
Atom 1	O(1A)	O(1B)	C(2A)	C(2B)	C(3A)	C(3B)
Atom 2	O(4A)	O(4B)	C(5A)	C(5B)	C(6A)	C(6B)
Atom 3	O(7A)	O(7B)	C(8A)	C(8B)	C(9A)	C(9B)
Atom 4	O(10A)	O(10B)	C(11A)	C(11B)	C(12A)	C(12B)
Atom 5[b]	(Na)	(Na)	(Na)	(Na)	(Na)	(Na)
m_1	0.505	0.879	0.543	0.896	0.508	0.928
m_2	−5.324	−5.460	−5.346	−5.480	−5.334	−5.472
m_3	22.552	22.447	22.537	22.434	22.546	22.435
d	1.218	−1.704	2.255	−2.727	1.692	−2.175
$\Delta d(1)$	0.004	−0.000	−0.013	0.011	−0.024	0.023
$\Delta d(2)$	−0.004	0.000	0.013	−0.011	0.024	−0.023
$\Delta d(3)$	0.004	−0.000	−0.013	0.011	−0.024	0.023
$\Delta d(4)$	−0.004	0.000	0.013	−0.011	0.024	−0.023
$\Delta d(5)$	(−1.497)	(1.505)	(−2.525)	(2.529)	(−1.969)	(1.987)

[a] See footnote *a* of Table VII. [b] Least-squares planes are determined by atoms 1–4.

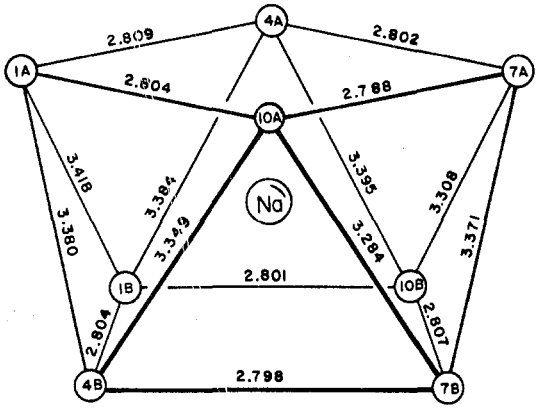

Figure 5. Dimension of the square antiprism formed by the oxygen atoms in the $[Na^+(C_8H_{16}O_4)_2]$ unit.

while the β carbons are associated with planes 2.525 and 2.529 Å away from sodium for A and B, respectively. The mean Na···C distances are 3.246 Å for the α carbons and 3.344 Å for the β carbons.

The parameters *s* and *l* of the square antiprism[15] average 2.802 and 3.361 Å, respectively, and the four classes of O-Na-O angles (Table VI) have mean values of 68.6, 85.1, 105.7, and 144.5°. The Na-O-C angles fall into two groups corresponding to the two types of carbon atoms. Their average values are 109.0° for C=C(α) and 115.3° for C=C-(β). These angles apparently serve to direct lone pair electrons from tetrahedrally hybridized oxygen atoms toward the cation. All of these parameters agree well with those determined for II.

The Tetraoxacyclododecane Ring. C_4 symmetry is respected closely by the 12-membered rings and provides a convenient basis for averaging their geometric parameters. Mean values for the three types of internal angles in the ring are C(α)-O-C(β) = 113.6°, O-C(α)-C(β) = 112.9°, and C(α)-C(β)-O = 107.9°. Torsional angles (Table VII) average −80.2° for the O-C(α) bonds, 163.2° for C(β)-O, and −58.7° for C(α)-C(β). These values agree closely with those observed for II and define a conformation that staggers the methylene hydrogens, brings four oxygens into close proximity to the cation, and directs the lone pair electrons toward the positive center. The eight C-C bond distances range from 1.476 to 1.502 Å (average 1.485 Å), while the 16 C-O bonds, which vary in length between 1.409 and 1.446 Å, have an average value of 1.424 Å.

Thermal Motion. The thermal parameters in the cyclomer-metal complex of I exhibit the same properties previously reported for II; the amplitudes of vibration and the degree of anisotropy are lowest for sodium, intermediate for oxygens, and highest for the carbons (Table II). In the aqueous layer W(6) exhibits the largest thermal amplitudes. The highest degree of anisotropy is displayed by the three-coordinated oxygen atoms W(3) and W(4), with the principal component directed along *x*. Interestingly, although W(1) and W(7) belong to the same topological class as W(3) and W(4), their thermal vibrations are more nearly isotropic. The unique oxygen W(5) shows the least anisotropy. The spiro-type atoms on the twofold axes display their largest thermal amplitudes in directions perpendicular to the diad (Figure 2).

Electrical Properties of the Complexes. The laminar structure of the crystals suggests some interesting possibilities regarding their electrical properties. The sodium ions form a layer which is separated from the layer of hydroxide ions by about 6 Å and insulated from it by the organic molecules. This arrangement reduces the coulombic interaction between oppositely charged ions, leaving them to move almost independently in their respective layers. The staggered arrangement of the cation complex precludes easy movement of the sodium ions from sandwich to sandwich should there be vacancies in the crystal. The arrangement of the hydroxide-water layer, on the other hand, is highly suitable for either hydroxide or proton migration. Such movement can be compared with that of ions in ice[16] but there are some interesting differences. Kelly and Salomon[17] have recently studied the electrical properties of ice doped with NaOH and have concluded that the hydroxide ion is substitutionally incorporated in the water lattice. Its presence produced both a Bjerrum L defect and a negative ion defect in the lattice[18]

The sodium ion is located interstitially and ion pairs strongly with its counterion, the dissociation constant being 10^{-10} to 10^{-12} *M*. The studies were limited to NaOH concentrations less than 10^{-5} *M* because of limited solubility. Under these conditions the free ion concentration was on the order of

(15) S. J. Lippard, *Progr. Inorg. Chem.*, 8 (1967).

(16) R. P. Auty and R. H. Cole, *J. Chem. Phys.*, 20, 1309 (1952).
(17) D. J. Kelly and R. E. Salomon, *J. Chem. Phys.*, 50, 75 (1969).
(18) N. Bjerrum, *Kgl. Dan. Vidensk. Selsk., Mat.-Fys. Medd.*, 27, 1 (1951); *Science*, 115, 385 (1952).

10^{-8} *M*. However, in the present case the water layer contains one hydroxide ion per eight water molecules corresponding to a concentration of about 7 *M*. As was described above, the location of the hydroxide ion is not known unambiguously and may be distributed over all oxygen positions. Chemically there are two types of positions, those where oxygen is bonded to four hydrogen atoms and those where oxygen is bonded to three hydrogens. In contrast to the ice structure, the hydroxide ion does not constitute a defect in either position; rather the extra proton which is not included in the H-bonded network might be considered a defect (which we will term an N defect or N site) since it involves a nonhydrogen bonding atom. We will now point out how this site can play an important role in conducting electricity through the water sheet.

The generally accepted mechanism for electrical conduction in ice involves the concurrent migration of ion defects and Bjerrum defects as shown in Figure 6a. The overall conductivity will be controlled by the less effective of the two migrations whose rates in turn are determined by the rates of migration of each defect and the number of defects.[14] The ion defect migration is extremely fast if all the hydrogen bonds are aligned properly since it involves only the transfer of a proton from one oxygen to the next within a hydrogen bond. The Bjerrum defect migration is slower since it involves the breaking of a hydrogen bond, rotation of a water molecule, and formation of a hydrogen bond. The result is that in ice doped with NaOH, the Bjerrum defect migration rate limits the conductivity.

In the water sheet of the NaOH complex both ion and Bjerrum defect migrations are possible, but in addition N-site migration offers another mode of reorienting the hydrogen bond structure. The latter should be very effective because of the very large number of sites (one for every nine oxygens) and because the energy barrier to migration should be smaller. The migration is shown schematically in Figure 6b. As a water molecule next to N site rotates, the N-site proton can simultaneously form a new hydrogen bond and the proton on the other side of the rotating molecule can move into the N-site position. It is, therefore, unnecessary to go through the conformation where two N bonds are broken to be replaced by Bjerrum L and D defects, as is the case in ice. Examination of Figure 3 shows that the four sites that can accommodate N defects, O(1), O(3), O(4), and O(7), are separated from each other by one tetrahedrally H-bonded site so that there is a continuous path for migration of the N site along the sheet. These agruments

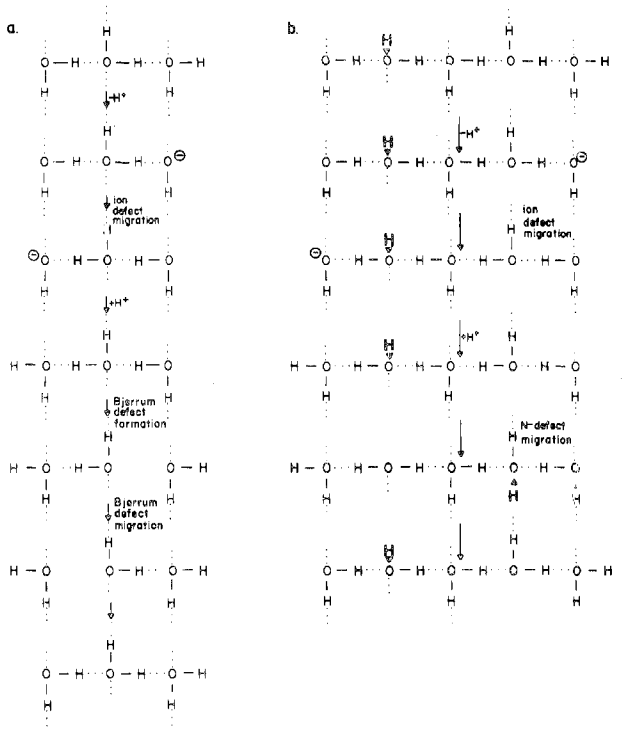

Figure 6. Schematic representation of the electrical conductivity in (a) ice; (b) the water layer in $[Na^+(C_8H_{16}O_4)_2][OH^-\cdot 8H_2O]$.

lead one to expect that crystals of the NaOH complex would have very high conductivity in directions parallel to the plane of the water sheet, but very low conductivity in the direction normal to the plane.

Acknowledgment. We thank P. P. North for assistance in gathering the X-ray intensity data and V. B. Carter for measurement and interpretation of ir and Raman spectra. We are also grateful to J. C. Evans for helpful discussions.

Registry No. $NaOH\cdot 2C_8H_{16}O_4\cdot 8H_2O$, 52540-77-9.

Supplementary Material Available. A listing of calculated and observed structure factor amplitudes will appear following these pages in the microfilm edition of this volume of the journal. Photocopies of the supplementary material from this paper only or microfiche (105 × 148 mm, 24× reduction, negatives) containing all of the supplementary material for the papers in this issue may be obtained from the Journals Department, American Chemical Society, 1155 16th St., N.W., Washington, D. C. 20036. Remit check or money order for $4.00 for photocopy or $2.00 for microfiche, referring to code number INORG-74-2826.